A Nucleotide-Analogue-Induced Gain of Function Corrects the Error-Prone Nature of Human DNA Polymerase iota

Amit Ketkar,[†] Maroof K. Zafar,[†] Surajit Banerjee,[‡] Victor E. Marquez,[§] Martin Egli,[¶] and Robert L. Eoff*[,†]

[†]Department of Biochemistry and Molecular Biology, University of Arkansas for Medical Sciences, Little Rock, Arkansas 72205-7199, United States

[‡]Northeastern Collaborative Access Team and Department of Chemistry and Chemical Biology, Cornell University, Building 436E, Argonne National Laboratory, Argonne, Illinois 60439, United States

[§]Chemical Biology Laboratory, Center for Cancer Research, National Cancer Institute at Frederick, Frederick, Maryland 21702, United States

[¶]Department of Biochemistry, Vanderbilt University School of Medicine, Nashville, Tennessee 37232-0146, United States

S *Supporting Information*

ABSTRACT: Y-family DNA polymerases participate in replication stress and DNA damage tolerance mechanisms. The properties that allow these enzymes to copy past bulky adducts or distorted template DNA can result in a greater propensity for them to make mistakes. Of the four human Y-family members, human DNA polymerase iota (hpol ι) is the most error-prone. In the current study, we elucidate the molecular basis for improving the fidelity of hpol ι through use of the fixed-conformation nucleotide North-methanocarba-2′-deoxyadenosine triphosphate (N-MC-dATP). Three crystal structures were solved of hpol ι in complex with DNA containing a template 2′-deoxythymidine (dT) paired with an incoming dNTP or modified nucleotide triphosphate. The ternary complex of hpol ι inserting N-MC-dATP opposite dT reveals that the adenine ring is stabilized in the *anti* orientation about the pseudo-glycosyl torsion angle, which mimics precisely the mutagenic arrangement of dGTP:dT normally preferred by hpol ι. The stabilized *anti* conformation occurs without notable contacts from the protein but likely results from constraints imposed by the bicyclo[3.1.0]hexane scaffold of the modified nucleotide. Unmodified dATP and South-MC-dATP each adopt *syn* glycosyl orientations to form Hoogsteen base pairs with dT. The Hoogsteen orientation exhibits weaker base-stacking interactions and is less catalytically favorable than *anti* N-MC-dATP. Thus, N-MC-dATP corrects the error-prone nature of hpol ι by preventing the Hoogsteen base-pairing mode normally observed for hpol ι-catalyzed insertion of dATP opposite dT. These results provide a previously unrecognized means of altering the efficiency and the fidelity of a human translesion DNA polymerase.
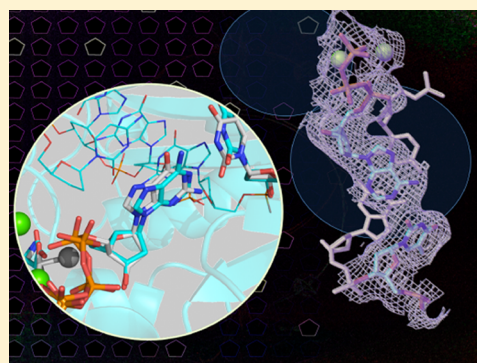
INTRODUCTION

Synthesis of nucleic acids is a fundamental process performed by all biological systems.[1] Nucleic acid polymerases catalyze nucleotidyl transfer using a two metal ion-dependent mechanism that relies upon deprotonation of the nucleophilic 3′-OH group at the primer terminus, with subsequent protonation of the pyrophosphate leaving group from the incoming nucleotide triphosphate.[2] A precise arrangement of catalytic groups must be achieved for successful nucleic acid synthesis to occur. Multiple kinetic and structural checks upon replication fidelity have been identified that ensure faithful replication of the genome.[3] Moreover, the efficiency and fidelity of polymerase activity can have important ramifications upon genomic stability and cellular survival.[4−8] Chemical modification of either the DNA substrate or the incoming dNTP can modulate catalytic rates of polymerases but in some instances these alterations may also serve as useful probes of factors that influence catalysis.[9−12] Despite the apparent universality of general acid catalysis by polymerases there are many features related to nucleotide geometry/chemistry and substrate recognition by unique polymerase active sites that ultimately yield a variety of observed catalytic properties among different polymerase subfamilies. Perhaps nowhere is the mechanistic diversity of DNA synthesizing enzymes more apparent than with the Y-family DNA polymerases.

Y-family DNA polymerases are conserved evolutionarily from prokaryotes through eukaryotic systems as an apparent means of tolerating damage to the genome and in the replication of non-B-form DNA.[6,13−15] In bacteria, the Y-family pols participate in the so-called SOS response to DNA damage and/or replication stress, with a similarly effective means of regulation and recruitment occurring in eukaryotes.[16] Once the genes associated with damage responses had been identified as

DNA polymerases, functional studies reported an intriguing ability of the Y-family pols to bypass DNA adducts, often with relatively unperturbed efficiency.[17−21] The classic example of polymerase specific translesion DNA synthesis is the accurate and efficient bypass of UV-induced cyclobutane pyrimidine dimers by polymerase η.[21] The biological relevance of the Y-family is highlighted in the skin cancer prone disease xeroderma pigmentosum variant (XPV), which results from mutations in the human RAD30 gene that codes for pol η.[8] Additional studies indicate that Y-family DNA polymerases are dysregulated in several types of cancer, including brain, colorectal, and non-small-cell lung cancers, though the exact contribution of these enzymes to tumor-associated genomic instability and/or tumor progression remains poorly defined.[22−24]

It is apparent from *in vitro* functional assays that the fidelity of the Y-family pols is diminished relative to replicative pols, such as those found in the A- and B-families.[25,26] Structural work reported during the past 12 years, primarily in the form of X-ray crystallographic analysis, has revealed the molecular details of Y-family DNA polymerases in complex with many different DNA adducts.[27] DNA adducts of varying sizes and unusual base-pairing modes have been observed in the active sites of the Y-family polymerases, supporting the notion that these enzymes are tolerant of damaged template DNA. Additionally, these structures have provided a basis for understanding why nucleotide selection by the Y-family is more promiscuous than other polymerase families. All of the Y-family pols studied have active sites that lack stringent checks upon base-pairing fidelity and are more solvent exposed than the higher fidelity replicative counterparts.[27] The uniqueness of the Y-family lies not only in the ability to bypass DNA damage but also in the diversity of mechanisms used to perform catalysis opposite bulky chemical additions or distorted template strands (e.g., protein template-directed DNA synthesis and Hoogsteen base-pairing modes).[28,29] Ultimately, it is the ability of these enzymes to accommodate or stabilize non-canonical nucleic acid structures during DNA synthesis that makes them valuable "assets" to biological systems. The current work sought to discover the molecular basis for improving the fidelity of a human Y-family member, namely DNA polymerase iota.

The Y-family member human DNA polymerase iota (hpol ι) is highly error-prone on undamaged DNA.[30−32] Unique structural attributes contribute to the bypass properties of hpol ι, as well as its low fidelity. Like other Y-family members, hpol ι possesses a solvent exposed active site. However, the C1′−C1′ distance between the template residue and the incoming dNTP is consistently constrained to ∼8−9 Å in the active site of hpol ι, which is ∼1−2 Å narrower than what is observed for Watson−Crick base pairs. The narrowed width between the template and the incoming dNTP leads to an unusual propensity to form Hoogsteen-type base pairs in the hpol ι active site during bypass of both damaged and undamaged template purines.[29,33−35] However, the preferential use of Hoogsteen base pairs is noticeably altered when hpol ι copies a template 2′-deoxythymidine (dT).[36] Normally, hpol ι incorporates dGTP opposite template dT approximately 10−15-fold more efficiently than dATP.[32,37] The structural rationale for the preferential incorporation of dGTP was deduced from crystal structures that showed the incoming guanine ring stabilized with an *anti* glycosyl torsion angle (χ = −159°) through a hydrogen bond with Gln59 of hpol ι.[36] In a separate study, our group showed that the error-prone nature of

hpol ι-catalyzed bypass of thymidine could be alleviated by utilizing North-methanocarba-2′-deoxyadenosine triphosphate (N-MC-dATP).[37] N-MC-dATP is a fixed-conformation nucleotide analogue that mimics furanose geometry for "North"-type sugar puckers.

When used to describe the properties of five-membered furanose ring systems, the terms North and South are related to a value called the pseudorotation phase angle (P) that, when combined with the amplitude of puckering (ν_{max} or τ_m), defines the overall geometry of the five torsion angles of the furanose ring of ribose and 2′-deoxyribose. By convention, a P value equal to 0° sits a top a pseudorotation wheel and is said to reside in the "Northern" (N) quadrant of the cycle (Figure 1),
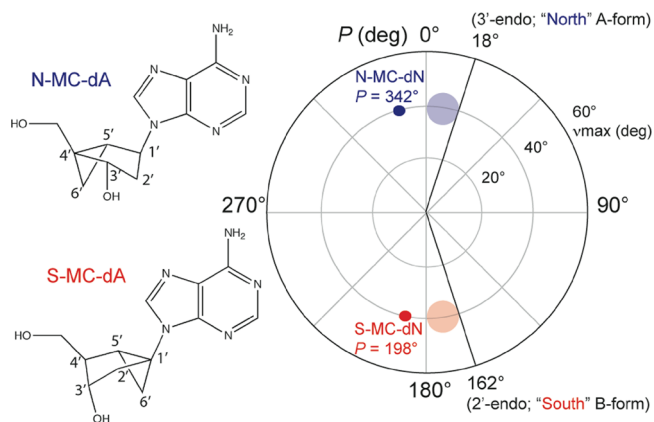

Figure 1. Chemical structures of N-MC-dA and S-MC-dA shown alongside the pseudorotational cycle to compare the N/S-MC conformations with C3′-endo and C2′-endo puckers most common to RNA and DNA helices, respectively. The semi-transparent circles indicate the clustering of C3′-endo (blue) and C2′-endo (red) conformations of ribose and 2′-deoxyribose moieties.

with P equal to 180° identified as the "Southern" (S) antipode. The bicyclo[3.1.0]hexane scaffold of the fixed conformation nucleotide analogues used here substitute for 2′-deoxyribose and effectively locks the "pucker" of the furanose mimic into a geometry that resembles either the C3′-endo sugar pucker most commonly observed in A-form helices (North) or C2′-endo pucker observed in B-form helices (South) (Figure 1).[38,39] These compounds were originally developed as delayed chain terminators of viral replication and as probes of furanose conformational preferences in the active sites of enzymes.[40,41] An increase in hpol ι-activity was unexpected as most polymerases tested were inhibited to some extent by the fixed conformation N-MC-dATP. In the present work, we elucidate the structural basis for the correction of hpol ι fidelity during insertion of fixed conformation nucleoside analogues. Moreover, our structures are the first reported for any polymerase bound to either N-MC-dATP or S-MC-dATP. The results provide a framework for understanding the molecular determinants that alter the error-prone nature of hpol ι and could prove useful in designing new compounds to modulate the activity of translesion DNA polymerases.

■ MATERIALS AND METHODS

Materials. 2′-Deoxy-adenosine triphosphate was obtained from GE Healthcare Life Sciences (Piscataway, NJ). All oligonucleotides used in this work were synthesized by Integrated DNA technologies (Coralville, IA) and purified using HPLC by the manufacturer, with analysis by matrix-assisted laser desorption time-of-flight MS. A self-
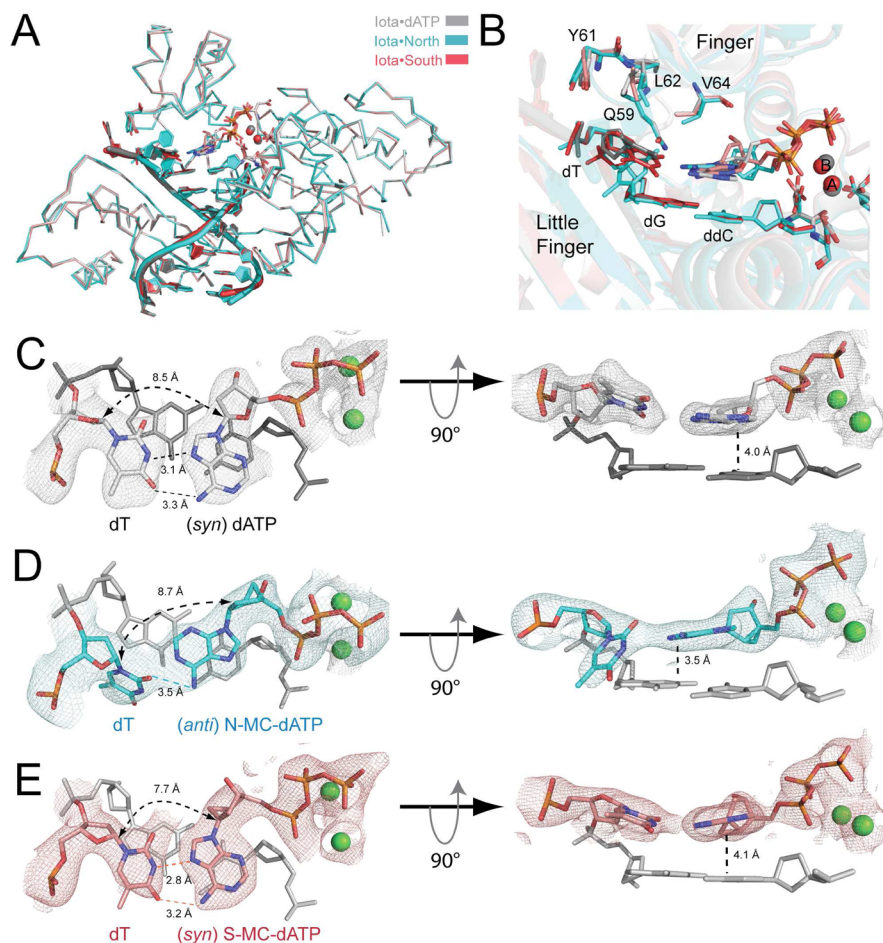
Figure 2. The hpol ι ternary complexes and active-site electron densities reveal nucleotide analogue induced changes in the formation of nascent base pairs. (A) Superimposition of the three hpol ι structures reveals similar overall protein conformation (rmsd ≈ 0.4 Å). Iota·dATP (gray), iota·North (cyan) and iota·South (light red) complexes are shown with protein in ribbon form and the DNA in cartoon form. Spheres represent calcium ions. The incoming dNTP is shown in stick form. (B) The active-site interactions for the three structures are superimposed upon one another using the same color scheme as in panel A. The orientations of the nascent base pair in the (C) iota·dATP (white), (D) iota·North (cyan), and (E) iota·South (light red) complexes are shown with the $2F_o − F_c$ density map (wire mesh) contoured to 1σ around the nascent base pair and active-site metal ions. Hydrogen bonding patterns and the C1′−C1′ distances are noted in each panel. The active-site view is rotated 90° to show the relative orientation of each nascent base pair and the primer−template junction (gray nucleotides). The average base-stacking distance between the incoming adenine and the primer−template base pair is noted.

annealing 18-mer with a 2′,3′-dideoxy-terminated 3′-end was used for crystallization (5′-TCC TGG GTC CTA GGA CCCdd-3′). The nucleoside analogues North-methanocarba-2′-deoxyadenosine (N-MC-dA) and South-methanocarba-2′-deoxyadenosine (S-MC-dA) were synthesized as described previously[42] and converted to the triphosphate form by TriLink BioTechnologies (San Diego, CA).

Protein Purification, Crystallization, and Structure Determination. The core polymerase domain of hpol ι (residues 1−420) was expressed and purified as described previously.[35] The highly pure hpol ι-core protein was stored at −80 °C in the HEPES buffer (pH 7.5) containing 0.1 M NaCl, 5 mM 2-mercaptoethanol, and 30% glycerol, at a final concentration of 25 mg/mL. Crystals for the hpol ι$_{1−420}$ complexes with N-MC-dATP and S-MC-dATP were obtained by the sitting drop vapor diffusion method in a reservoir solution of 20 mM Tris-HCl (pH 7.3 at 22 °C) buffer containing 5% glycerol, 10 mM 2-mercaptoethanol, 0.15 M CaCl₂, and 12% PEG 3350. Crystals for the hpol ι$_{1−420}$ complexes with dATP were obtained by the sitting drop vapor diffusion method in a reservoir solution of 20 mM Tris-HCl (pH 7.3 at 22 °C) buffer containing 5% glycerol, 10 mM 2-mercaptoethanol, 0.25 mM MK-886, 0.15 M CaCl₂, and 10% PEG 3350. For obtaining crystals of hpol ι$_{1−420}$ with N-MC-dATP, S-MC-dATP, and dATP, purified hpol ι$_{1−420}$, the double-stranded 18-mer self-annealing DNA substrate, and dATP or S-MC-dATP were

mixed in the molar ratio 1:1.2:4 containing 5 mM MgCl₂. Crystals were obtained in 24−48 h and were cryo-protected by serial soaking in mother liquor containing 10−25% glycerol, and were then flash-frozen in liquid nitrogen. For the North complex, binary complex crystals with hpol ι$_{1−420}$ and the self-annealing 18-mer dsDNA were soaked overnight in a solution containing 0.5 mM N-MC-dATP. The crystals were then cryo-protected in solutions containing N-MC-dATP and 10−25% glycerol, followed by flash-freezing in the same way as for the hpol ι$_{1−420}$ dATP/S-MC-dATP crystals. Data was collected at the Advanced Photon Source on the Northeastern Collaborative Access Team beamlines (Argonne, IL). Scaling and indexing of the data was performed using the HKL package in space group P6522 to a resolution of 2.90 Å (North), 2.57 Å (South) and 2.10 Å (dATP). The structures were solved by molecular replacement using the coordinates of the structure 3GV5 as the search model.[36] Only the protein and DNA atoms from the search model were used for molecular replacement. Refinement was performed with PHENIX and model building was carried out using COOT on the PHENIX platform.[43,44] Nucleic acid structural parameters were analyzed using 3DNA.[45,46] Crystallographic representations were prepared using PyMol (DeLano Scientific, San Carlos, CA).
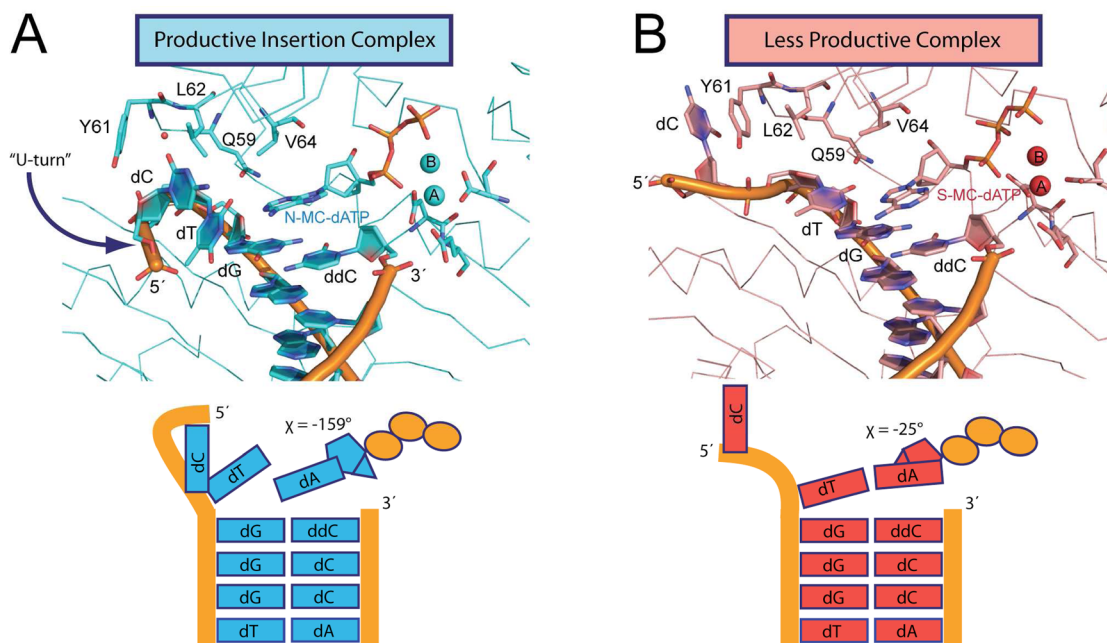
Figure 3. The active-site base-pairing mode correlates with alterations in the template DNA strand. (A) The catalytically favored pairing of *anti* N-MC-dATP:dT in the iota·North structure is shown in cartoon form. This productive nascent base pair is observed with the pronounced bend in the template DNA (U-turn). (B) The less productive *syn* S-MC-dATP:dT base pair in the iota·South structure is shown in cartoon form to illustrate the orientation of the template strand. A schematic illustration of the nucleic acid conformations and base-pairing modes is shown below each panel.

■ RESULTS AND DISCUSSION

Unmodified dATP Forms a Hoogsteen Base Pair with Template dT. The most striking result from our previous work with fixed-conformation nucleotide analogues was observed with hpol ι, which showed increased catalytic activity for N-MC-dATP relative to unmodified dATP when inserting opposite template dT. The catalytic efficiency ($k_{cat}/K_{m,dNTP}$) for N-MC-dATP insertion was similar to that measured for dGTP insertion opposite dT, which is the preferred mode of hpol ι-catalyzed bypass of dT. However, the mechanistic basis for the alteration in hpol ι fidelity remained unclear. In order to identify the molecular rationale for the unusual catalytic properties of hpol ι we set out to solve a series of crystal structures with the polymerase in complex with fixed-conformation nucleotide analogues. However, as previous structures reported conflicting results,[36,47] we first sought to determine the structure of dATP paired with template dT in the active site of hpol ι.

Three crystal structures were solved of hpol ι in ternary complex with DNA and an incoming dNTP or MC-dNTP (see Supporting Information Table S1). Superimposition of the three structures reported reveals essentially no change in the conformation of the protein (Figure 2A). There are three metal ions in each of the structures reported here: two metal ions near the active-site and one coordinated with amino acid side-chains in the thumb domain of hpol ι. The catalytic and coordinating metal ions in the active site are labeled (A) and (B), respectively (Figure 2B). These metal ions were refined as calcium since the crystallization buffer contained 150 mM $CaCl_2$. As noted, the ternary complex of hpol ι in complex with an incoming adenosine (dATP and ddADP) has been reported twice before, with conflicting results.[36,47] Our structure is consistent with the pairing mode observed for ddADP:dT (pdb ID 3GV5),[36] with the difference being that we used dATP, our primer terminus is dideoxy-terminated and our DNA differs

slightly in sequence. Previously, density was only observed for α and β phosphates of ddADP but there is clear density for all three phosphates in our structure (Figure 2C). Importantly, in both our iota·dATP structure and in the ddADP:dT structure (pdb ID 3GV5), the glycosyl torsion angle (χ) of adenosine resides in the *syn* orientation ($\chi = -25.2°$ for dATP), which presents a Hoogsteen-type base-pairing scheme (Figure 2C). The *syn* orientation of the adenine increases the average distance between purine ring system and the primer terminus to around 4 Å and is consistent with weakened base-stacking interactions for the incoming dATP. The ribose pucker is clearly in the C2′-endo (South) orientation for dATP in our structure, with the 3′-OH group directed toward the primer–template junction. Such an orientation for the 3′-OH group would be highly inhibitory to extension. Like previous hpol ι structures, the C1′–C1′ distance is narrowed to 8.5 Å between dATP and dT (Figure 2C). A notable difference between our hpol ι dATP:dT structure and the ddADP:dT structure reported by others resides in the template DNA where we do not observe the pronounced curvature of the template strand ("U-turn") that was previously proposed to inhibit extension.[36] Instead, the template strand 5′ of the nascent base pair extends between the finger and little finger domains. In all three of our structures, the side chain of Tyr61 remains flipped into the orientation observed previously, which stacks perfectly against the pyrimidine ring of dC just 5′ of template dT (Figure 2B). Using the iota·dATP and ddADP:dT structures as points of reference, we then went on to analyze the binding mode for N-MC-dATP and S-MC-dATP in the active site of hpol ι.

Molecular Rationale for the Improvement of hpol ι Fidelity. The iota·North structure of hpol ι in complex with DNA and a nascent N-MC-dATP:dT base pair immediately suggests the molecular basis for increased activity. The N-MC-dATP pseudo-glycosyl bond is clearly observed in the *anti* orientation (Figure 2D; $\chi = -159°$), which is in direct contrast

to the less productive *syn* orientation observed for dATP. Maintaining the adenine ring of N-MC-dATP in the *anti* conformation causes dT to shear 2 Å out of plane with the adjacent bases. Notably, there is only one hydrogen bond between the incoming N-MC-dATP and template dT. The N6 amino group of N-MC-dATP appears to form a weak hydrogen bond (3.5 Å) with the O2 atom of template dT (Figure 2D). The single H-bond between N-MC-dATP and dT is in contrast to the two hydrogen bonds observed between the N6 and N7 positions of Hoogsteen oriented (*syn*) dATP and the N3 and O4 atoms, respectively, of template dT in our iota·dATP structure (Figure 2C,D). The lack of hydrogen bonding stabilization in what is a catalytically productive N-MC-dATP:dT base-pairing indicates a more influential role for additional factors during hpol ι catalysis. The base-stacking interactions between N-MC-dATP and the primer−template junction (ddC:dG; Figure 2C, gray bases) are more extensive than those observed in the dATP:dT Hoogsteen pair. There is an average distance near 3.5 Å between the adenine ring of N-MC-dATP and the template dG, whereas the adenine ring of dATP hovers over the primer terminal ddC at a distance closer to 4 Å. Again, three metal ions (Figure 2; Ca^{2+}) are found in the iota·North complex, with the catalytic ion loosely coordinated by active site side chains. The dideoxy-terminated primer terminus is perfectly positioned in a productive mode ~4 Å from the α phosphate. Interestingly, the template strand in the iota·North structure adopts the "U-turn" conformation (Figure 3A). Thus, the iota·North structure is distinct from unmodified dATP and as will be discussed, very closely resembles the binding mode of dGTP paired opposite dT.

Similar to dATP, S-MC-dATP Is Bound in the hpol ι Active Site in a Nonproductive Fashion. Next, the active site of hpol ι in complex with a S-MC-dATP:dT nascent base pair was determined (iota·South). Similar to dATP, the adenine ring of S-MC-dATP is placed into the *syn* orientation about the pseudo-glycosyl bond to form two hydrogen bonds with template dT in a Hoogsteen pairing mode (Figure 2E). The phosphates are coordinated in a manner that is identical to dATP and N-MC-dATP but the remainder of the S-MC-dATP molecule is shifted ~2 Å out of the active site cleft relative to N-MC-dATP (Figure 4A). There is essentially no variation in the distance between the C3′ atom of the dideoxycytosine (ddC) and the α phosphate for the three structures reported here. All of the structures show a distance near 4 Å, which should be optimal for phosphoryl transfer. The α phosphate of N-MC-dATP is 4.0 Å from the C3′ atom of ddC, whereas S-MC-dATP and dATP are 4.1 Å, a difference of 0.1 Å that is limited by the resolution of the data. The incoming dGTP paired with dT that was solved previously at a resolution of 2.0 Å is positioned with the α phosphate 3.8 Å from the C3′ atom of ddC.[36]

The base-stacking distance between S-MC-dATP and the primer terminus is near 4 Å, similar to dATP and weaker than that observed for N-MC-dATP, while the C1′−C1′ distance is slightly shorter (~1 Å) than in the other two complexes at 7.7 Å (Figure 2E). Similar to the iota·dATP structure, the template strand 5′ of the nascent base pair does not appear to adopt the U-turn but instead stacks well with Tyr61 and resides between the finger and little finger domains (Figure 3B). It is important to note that both of the catalytically less productive molecules (dATP and S-MC-dATP) form a Hoogsteen base pair with dT in the hpol ι active site, whereas the productive N-MC-dATP exposes the Watson−Crick face of the incoming dNTP to the
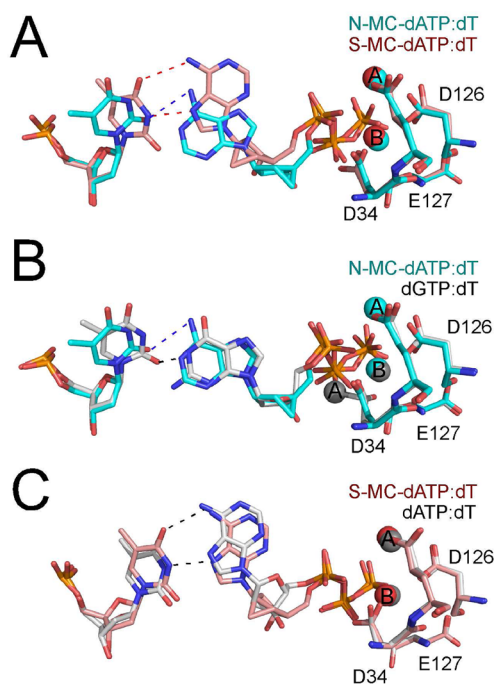
Figure 4. Comparative view of the base-pairing modes for MC-dATP molecules in the active site of hpol ι. (A) Superimposition of the base pairs observed in the iota·North (cyan) and iota·South (light red) structures. (B) Superimposition of iota·North (cyan) and hpol ι pairing dGTP and dT (white, pdb ID 3GV8). (C) Superimposition of iota·South (light red) and iota·dATP (white). Dashed lines denote hydrogen bonds. Active-site catalytic residues are noted, as are the presumed catalytic and coordinating calcium ions (labeled A and B, respectively).

template dT (Figure 4B,C). The formation of two hydrogen bonds between the less productive Hoogsteen base pairs again illustrates the fact that electrostatic interactions play a minimal role in stabilizing the nascent base pair in the active site of hpol ι, as both N-MC-dATP:dT and dGTP:dT base pairs are stabilized by a single hydrogen bond (Figure 4B).

N-MC-dATP Is Bound to the hpol ι Active Site in a Manner That Is Virtually Identical to dGTP. Steady-state kinetic analysis of single nucleotide insertion by hpol ι shows that dGTP is inserted ~10−15-fold more efficiently than dATP opposite template dT.[32,37] The structure of hpol ι bound to an incoming dGTP paired with dT (pdb code 3GV8) revealed distinct contacts that were thought to promote selection of dGTP over dATP.[36] First, an electrostatic interaction between the N2 exocyclic group of dGTP and Glu59 appeared to stabilize the incoming nucleotide triphosphate in an *anti* orientation. Also, the stabilization of *anti* dGTP deep in the narrowed active-site pocket causes the template dT to shear 1.7 Å out of plane (Figure 4B). This distortion of the template base paired opposite dGTP is large compared to the 0.4 Å shear observed for template dT paired with dATP (Figure 2C). However, it is virtually identical to what is observed for N-MC-dATP:dT (Figure 4B). Intriguingly, there are no apparent electrostatic contacts that stabilize the adenine ring of N-MC-dATP in the *anti* orientation. Yet, it is this feature that appears to explain the increased catalytic efficiency of hpol ι. The stabilized *anti* conformation results in faster insertion than unmodified dATP, as evidenced by an increased turnover number for N-MC-dATP[37] and also improves the accuracy of hpol ι DNA synthesis opposite dT by increasing the propensity

of the enzyme to pair adenine with thymidine. Interestingly, the crystal structure of hpol ι inserting dGTP opposite dT reveals that the incoming dGTP resides in a "Western" type O4′-exo pucker (P = 271.2°). N-MC-dATP is locked into a pucker that is in the Northwestern quadrant of the pseudorotation cycle (P = 342°), which indicates another close similarity between our iota·North structure and the dGTP:dT base-pairing mode. In the absence of protein−nucleic acid contacts that stabilize N-MC-dATP in the *anti* orientation, it would appear that the chemical modifications used to immobilize the bicyclo[3.1.0]-hexane ring geometry also effectively lock the pseudo-glycosyl torsion angle in the *anti* conformation.

Altered Template DNA Orientation in Productive Complexes. It is worth noting that we only observe the U-turn in the template strand of our most productive complex, namely iota·North (Figure 3A). In the less catalytically competent iota·dATP and iota·South structures the template strand flips away from the DNA binding cleft and resides between the finger and little finger domains (Figure 3B). This is not to say that previous observations of the U-turn are incorrect or without merit. Indeed, the structures reported previously are most certainly accurate and of high quality. The previous paper used two different DNA sequences for crystallization. The first sequence (9 nt primer/15 nt template) places a dT residue on the 5′ side of the nascent ddADP:dT base pair. The second sequence used a self-annealing, dideoxy-terminated 18-mer similar in sequence to the one used here, except that a dA residue is positioned 5′ of dT in the 0 position (i.e., the nascent base pair). The U-turn was observed in both sequences. The oligonucleotide used in our crystallization conditions places a dC on the 5′ side of the 0 position dT. Previous experiments showed that stalling opposite dT seems to be sequence independent,[32] so the sequence used in our crystallization conditions is unlikely to have contributed to the lack of the U-turn. It appears likely that, in the case of our iota·dATP and iota·South structures, we have simply captured hpol ι in a state that occurs prior to formation of the U-turn.

■ CONCLUSIONS

Fixed-conformation nucleotide analogues were originally developed in order to circumvent excision-mediated resistance to nucleoside and nucleotide reverse transcriptase inhibitors.[40,41] These compounds can be inserted and then extended a few nucleotides prior to replication termination.[40,48] They have been used successfully as antivirals by utilizing the mechanism of delayed chain termination.[38,41,42,49] The methanocarba scaffolds employ a bicyclo[3.1.0]hexane ring system as a means of locking or "fixing" the furanose mimic into either a "North" (RNA-like) or "South" (DNA-like) ring geometry.[41] Previous work has examined the conformational preferences of the furanose ring system for different enzyme classes, including three human Y-family DNA polymerases.[37,42] A general conclusion was that polymerases tend to favor C3′-endo, North puckers over C2′-endo, South puckers for the incoming dNTP. However, insertion of MC-dNTPs tends to diminish catalytic efficiencies for most polymerases tested. Surprisingly, the highly error-prone hpol ι exhibited increased catalytic efficiency and fidelity when inserting the potent antiviral compound N-MC-dATP opposite a template dT. The bicyclo[3.1.0]hexane scaffold of N-MC-dATP has a predicted pseudorotation angle (P) near 342°, which mimics C3′-endo furanose geometry and normally inhibits replication by acting as a delayed chain terminator. The current study sought to

understand the molecular basis for altered fidelity of hpol ι in the presence of the fixed conformation nucleotide analogue N-MC-dATP. Uniquely, N-MC-dATP acts as an enhancer of hpol ι activity and fidelity. By understanding the molecular determinants that alter the error-prone nature of hpol ι we hoped to gain novel insights into fundamental aspects of specialized replication components, which might prove useful in designing new compounds to modulate the activity of these enzymes.

Our crystal structures reveal precisely why N-MC-dATP "corrects" the error-prone nature of hpol ι. Superimposition of N-MC-dATP:dT with dGTP:dT shows incredible similarity between the two active site base-pairing orientations (Figure 4B). In the latter instance, the binding of dGTP is stabilized by an electrostatic interaction between the N2 exocyclic amino group of deoxyguanine and Gln59 in the finger domain of hpol ι. No such interaction is found in the structure of hpol ι bound to N-MC-dATP (Figure 3A). Nonetheless, the purine ring of the incoming N-MC-dATP is held in the *anti* orientation, sitting in what is clearly a productive binding mode deep in the active site of hpol ι. Stabilization of the *anti* conformation for N-MC-dATP does not depend upon interactions with hpol ι. Instead, the geometric constraints imposed by the North methanocarba moiety shifts the *anti/syn* equilibrium in favor of the *anti* orientation. Both experimental evidence and calculated relative energies for different conformers of N-MC-2′-deoxyguanosine indicate that the *anti* conformer is stabilized by the fusion of cyclopropane ring through the C4′ position and that this stabilization is greater than that of unmodified dG.[50] A similar phenomenon was observed for the thymidine analogue (N-MC-dT)[42] and appears to be true for the N-MC-dATP derivative. However, this is not to say that the χ values for N-MC-dNTPs are more rotationally restricted by free energy barriers than S-MC-dNTPs. In fact, the S-type bicyclo[3.1.0]hexane ring system imposes a higher free energy barrier (∼2−3 kcal/mol) against rotation about χ than N-MC-dATP.[51] The rotation around the glycosyl bond to the *syn* orientation that is observed for S-MC-dATP is, therefore, not due to an inherent increase in the conformational flexibility for the modified nucleotide but rather a steep energetic barrier against rotation away from the *syn* conformation. The enhanced activity of hpol ι with N-MC-dATP can be attributed, at least in part, to the stabilization of the pseudo-glycosyl torsion angle by conformational restraints that are imposed by the bicyclo[3.1.0]hexane ring. Thus, locking the geometry of the ribose-mimic effectively locks the purine ring into the *anti* conformation, which in turn results in more stable and productive binding of N-MC-dATP at the active site of hpol ι. It is also noteworthy that the template DNA in the iota·North structure adopts the U-turn conformation observed for hpol ι bound to a dGTP:dT base pair. In both instances (N-MC-dATP:dT and dGTP:dT) the template thymidine is sheared out of plane with the adjacent base pair, much more so than for *syn* oriented dATP or S-MC-dATP (Figure 4). It appears that forming the U-turn in response to the relative positioning of an *anti* oriented dNTP in the active site of hpol ι may help stabilize the nascent base pair and improve the catalytic efficiency of insertion opposite dT but that this pronounced bending of the template strand is then inhibitory to extension.

DNA damage and replication stress responses are key barriers to tumorigenesis that if not regulated properly, can exacerbate the rampant genomic instability observed in many

cancers. The ability to modulate specialized DNA replication components, such as the Y-family polymerases, represents a unique opportunity to target enzymes that are central to mechanisms of chemo- and/or radio-resistance in certain tumors. However, targeted modulation of specialized enzymes is best effected when a structural rationale for the design of effective agents is available. Our current investigation illustrates the structural basis of alterations in hpol ι action by the fixed-conformation nucleoside analogue N-MC-dATP. The structures are the first of any polymerase to be captured in ternary complex with MC-dNTPs. Most interestingly, the geometric constraints imposed by chemical modification of the furanose ring in N-MC-dATP produce a molecule that is ideally suited to the active site of hpol ι during synthesis opposite dT. To our knowledge, the results reported here represent the first instance in which the activity and fidelity of a Y-family DNA polymerase have both been increased by use of a chemically modified substrate.

ASSOCIATED CONTENT

Supporting Information

Table summarizing the crystallographic data and refinement parameters. This material is available free of charge via the Internet at http://pubs.acs.org. The atomic coordinates and structure factors (codes 4EBC, 4EBD, and 4EBE for iota·North, iota·South and iota·dATP, respectively) have been deposited in the Protein Data Bank, Research Collaboratory for Structural Bioinformatics, Rutgers University, New Brunswick, NJ (http://www.rscb.org/).

AUTHOR INFORMATION

Corresponding Author
rleoff@uams.edu
Notes
The authors declare no competing financial interest.

ACKNOWLEDGMENTS

REFERENCES

(1) Alberts, B. *Molecular biology of the cell*; 4th ed.; Garland Science: New York, 2002.
(2) Castro, C.; Smidansky, E. D.; Arnold, J. J.; Maksimchuk, K. R.; Moustafa, I.; Uchida, A.; Gotte, M.; Konigsberg, W.; Cameron, C. E. *Nat. Struct. Mol. Biol.* **2009**, *16*, 212−8.
(3) Joyce, C. M.; Benkovic, S. J. *Biochemistry* **2004**, *43*, 14317−24.
(4) Bielas, J. H.; Loeb, K. R.; Rubin, B. P.; True, L. D.; Loeb, L. A. *Proc. Natl. Acad. Sci. U.S.A.* **2006**, *103*, 18238−42.
(5) Daee, D. L.; Mertz, T. M.; Shcherbakova, P. V. *Proc. Natl. Acad. Sci. U.S.A.* **2009**, *107*, 157−62.
(6) Friedberg, E. C.; Wagner, R.; Radman, M. *Science* **2002**, *296*, 1627−30.
(7) Loeb, L. A.; Monnat, R. J., Jr. *Nat. Rev. Genet.* **2008**, *9*, 594−604.
(8) Masutani, C.; Kusumoto, R.; Yamada, A.; Dohmae, N.; Yokoi, M.; Yuasa, M.; Araki, M.; Iwai, S.; Takio, K.; Hanaoka, F. *Nature* **1999**, *399*, 700−4.
(9) Guengerich, F. P. *Chem. Rev.* **2006**, *106*, 420−52.
(10) Bergen, K.; Steck, A. L.; Strutt, S.; Baccaro, A.; Welte, W.; Diederichs, K.; Marx, A. *J. Am. Chem. Soc.* **2012**, DOI: http://dx.doi.org/10.1021/ja3017889.
(11) Irimia, A.; Eoff, R. L.; Pallan, P. S.; Guengerich, F. P.; Egli, M. *J. Biol. Chem.* **2007**, *282*, 36421−33.
(12) Loakes, D.; Gallego, J.; Pinheiro, V. B.; Kool, E. T.; Holliger, P. *J. Am. Chem. Soc.* **2009**, *131*, 14827−37.
(13) Goodman, M. F. *Annu. Rev. Biochem.* **2002**, *71*, 17−50.
(14) Ohmori, H.; Friedberg, E. C.; Fuchs, R. P.; Goodman, M. F.; Hanaoka, F.; Hinkle, D.; Kunkel, T. A.; Lawrence, C. W.; Livneh, Z.; Nohmi, T.; Prakash, L.; Prakash, S.; Todo, T.; Walker, G. C.; Wang, Z.; Woodgate, R. *Mol. Cell* **2001**, *8*, 7−8.
(15) Woodgate, R. *Genes Dev.* **1999**, *13*, 2191−5.
(16) Chang, D. J.; Cimprich, K. A. *Nat. Chem. Biol.* **2009**, *5*, 82−90.
(17) Boudsocq, F.; Iwai, S.; Hanaoka, F.; Woodgate, R. *Nucleic Acids Res.* **2001**, *29*, 4607−16.
(18) Choi, J. Y.; Angel, K. C.; Guengerich, F. P. *J. Biol. Chem.* **2006**, *281*, 21062−72.
(19) Choi, J. Y.; Eoff, R. L.; Pence, M. G.; Wang, J.; Martin, M. V.; Kim, E. J.; Folkmann, L. M.; Guengerich, F. P. *J. Biol. Chem.* **2011**, *286*, 31180−93.
(20) Eoff, R. L.; Irimia, A.; Egli, M.; Guengerich, F. P. *J. Biol. Chem.* **2007**, *282*, 1456−67.
(21) Johnson, R. E.; Prakash, S.; Prakash, L. *Science* **1999**, *283*, 1001−4.
(22) Albertella, M. R.; Lau, A.; O'Connor, M. J. *DNA Repair (Amst)* **2005**, *4*, 583−93.
(23) Lemée, F.; Bavoux, C.; Pillaire, M. J.; Bieth, A.; Machado, C. R.; Pena, S. D.; Guimbaud, R.; Selves, J.; Hoffmann, J. S.; Cazaux, C. *Oncogene* **2007**, *26*, 3387−94.
(24) Wang, H.; Wu, W.; Wang, H. W.; Wang, S.; Chen, Y.; Zhang, X.; Yang, J.; Zhao, S.; Ding, H. F.; Lu, D. *Neuro. Oncol.* **2010**, *12*, 679−686.
(25) Eoff, R. L.; Choi, J. Y.; Guengerich, F. P. *J. Nucleic Acids* **2010**, *2010*, 830473.
(26) Kunkel, T. A. *J. Biol. Chem.* **2004**, *279*, 16895−8.
(27) Yang, W.; Woodgate, R. *Proc. Natl. Acad. Sci. U.S.A.* **2007**, *104*, 15591−8.
(28) Nair, D. T.; Johnson, R. E.; Prakash, L.; Prakash, S.; Aggarwal, A. K. *Science* **2005**, *309*, 2219−22.
(29) Nair, D. T.; Johnson, R. E.; Prakash, S.; Prakash, L.; Aggarwal, A. K. *Nature* **2004**, *430*, 377−80.
(30) Tissier, A.; Frank, E. G.; McDonald, J. P.; Iwai, S.; Hanaoka, F.; Woodgate, R. *EMBO J.* **2000**, *19*, 5259−66.
(31) Tissier, A.; Frank, E. G.; McDonald, J. P.; Vaisman, A.; Fernandez de Henestrosa, A. R.; Boudsocq, F.; McLenigan, M. P.; Woodgate, R. *Biochem. Soc. Trans.* **2001**, *29*, 183−7.
(32) Tissier, A.; McDonald, J. P.; Frank, E. G.; Woodgate, R. *Genes Dev.* **2000**, *14*, 1642−50.
(33) Kirouac, K. N.; Ling, H. *Proc. Natl. Acad. Sci. U.S.A.* **2011**, *108*, 3210−5.
(34) Pence, M. G.; Blans, P.; Zink, C. N.; Hollis, T.; Fishbein, J. C.; Perrino, F. W. *J. Biol. Chem.* **2009**, *284*, 1732−40.
(35) Pence, M. G.; Choi, J. Y.; Egli, M.; Guengerich, F. P. *J. Biol. Chem.* **2010**, *285*, 40666−72.
(36) Kirouac, K. N.; Ling, H. *EMBO J.* **2009**, *28*, 1644−54.
(37) Eoff, R. L.; McGrath, C. E.; Maddukuri, L.; Salamanca-Pinzon, S. G.; Marquez, V. E.; Marnett, L. J.; Guengerich, F. P.; Egli, M. *Angew. Chem., Int. Ed.* **2010**, *49*, 7481−5.
(38) Marquez, V. E. *Nucleic Acids Symp. Ser. (Oxf)* **2004**, 11−2.

(39) Marquez, V. E.; Hughes, S. H.; Sei, S.; Agbaria, R. *Antiviral Res.* **2006**, *71*, 268−75.

(40) Boyer, P. L.; Julias, J. G.; Marquez, V. E.; Hughes, S. H. *J. Mol. Biol.* **2005**, *345*, 441−50.

(41) Shin, K. J.; Moon, H. R.; George, C.; Marquez, V. E. *J. Org. Chem.* **2000**, *65*, 2172−8.

(42) Marquez, V. E.; Ben-Kasus, T.; Barchi, J. J., Jr.; Green, K. M.; Nicklaus, M. C.; Agbaria, R. *J. Am. Chem. Soc.* **2004**, *126*, 543−9.

(43) Adams, P. D.; Afonine, P. V.; Bunkoczi, G.; Chen, V. B.; Davis, I. W.; Echols, N.; Headd, J. J.; Hung, L. W.; Kapral, G. J.; Grosse-Kunstleve, R. W.; McCoy, A. J.; Moriarty, N. W.; Oeffner, R.; Read, R. J.; Richardson, D. C.; Richardson, J. S.; Terwilliger, T. C.; Zwart, P. H. *Acta Crystallogr. D: Biol. Crystallogr.* **2010**, *66*, 213−21.

(44) Emsley, P.; Lohkamp, B.; Scott, W. G.; Cowtan, K. *Acta Crystallogr. D: Biol. Crystallogr.* **2010**, *66*, 486−501.

(45) Lu, X. J.; Olson, W. K. *Nucleic Acids Res.* **2003**, *31*, 5108−21.

(46) Lu, X. J.; Olson, W. K. *Nat. Protoc.* **2008**, *3*, 1213−27.

(47) Jain, R.; Nair, D. T.; Johnson, R. E.; Prakash, L.; Prakash, S.; Aggarwal, A. K. *Structure* **2009**, *17*, 974−80.

(48) Boyer, P. L.; Vu, B. C.; Ambrose, Z.; Julias, J. G.; Warnecke, S.; Liao, C.; Meier, C.; Marquez, V. E.; Hughes, S. H. *J. Med. Chem.* **2009**, *52*, 5356−64.

(49) Prichard, M. N.; Keith, K. A.; Quenelle, D. C.; Kern, E. R. *Antimicrob. Agents Chemother.* **2006**, *50*, 1336−41.

(50) Saneyoshi, H.; Mazzini, S.; Avino, A.; Portella, G.; Gonzalez, C.; Orozco, M.; Marquez, V. E.; Eritja, R. *Nucleic Acids Res.* **2009**, *37*, 5589−601.

(51) Marquez, V. E.; Russ, P.; Alonso, R.; Siddiqui, M. A.; Shin, K. J.; George, C.; Nicklaus, M. C.; Dai, F.; Ford, H., Jr. *Nucleosides Nucleotides* **1999**, *18*, 521−30.